AC Induced Corrosion of Underground Steel Pipelines. Faradaic Rectification under Cathodic Protection: II. Theoretical Approach with Electrolyte Resistance and Double Layer Capacitance for Bi-Tafelian Corrosion Mechanism

Ibrahim Ibrahim, Michel Meyer, Hisasi Takenouti, Bernard Tribollet

http://dx.doi.org/10.5935/0103-5053.20150302

J. Braz. Chem. Soc., Vol. 27, No. 3, 605-615, 2016.
Printed in Brazil - ©2016 Sociedade Brasileira de Química
0103 - 5053 $6.00+0.00

Article

AC Induced Corrosion of Underground Steel Pipelines. Faradaic Rectification under Cathodic Protection: II. Theoretical Approach with Electrolyte Resistance and Double Layer Capacitance for Bi-Tafelian Corrosion Mechanism

Ibrahim Ibrahim,[a,c] Michel Meyer,[b] Hisasi Takenouti[*,c,d] and Bernard Tribollet[c,d]*

[a]*Al-Andalus University, Tartus, Al Qadmus, Syria*

[b]*GDFSUEZ, 93211 Saint Denis La Plaine, France*

[c]*Laboratoire Interfaces et Systèmes Electrochimiques (LISE), Sorbonne Universités, Université Paris 06, UMR 8235, 75005 Paris, France*

[d]*CNRS, UMR 8235, 75005 Paris, France*

AC corrosion enhancement of buried steel pipe is induced by high stray AC electromagnetic field and to the faradaic rectification due to non-linearity of current-potential characteristics. In Part I, this phenomenon was evaluated by neglecting the electrical resistance of soil electrolyte. In this part, we will examine when this resistance is no longer negligible. The mathematical model can be expressed by an ordinary nonlinear differential equation. In this part, the corrosion mechanism is modelled by two reactions obeying Tafel law, one for anodic dissolution of steel and another for cathodic process. This corrosion mechanism is valid when the corrosion current density is much higher than the diffusion limited current of dissolved oxygen. Compared with the system where the electrolyte resistance is negligible, the corrosion enhancement induced by AC signal is markedly attenuated because of the ohmic drop through the electrolyte resistance, and the double layer capacitance constitution a bypass circuit.

Keywords: electrolyte resistance, double layer capacitance, faradaic rectification, nonlinearity, digital simulation

Introduction

In Part I of this series of papers,[1] the mathematical development and digital simulations of AC voltage enhanced corrosion (or simply AC corrosion) on buried steel structures under the cathodic protection were reported for highly conducting electrolyte medium, that is, the contribution of the electrolyte resistance is negligible. In contrast, the cathodic process is more realistic than other publications,[2-7] since two reactions, the reduction of dissolved oxygen with partially diffusion limited process, and the water reduction according to a Tafel law were considered.[1,8] In this part, we will examine the AC enhanced corrosion when the solution resistance is no longer negligible. Then, the sinusoidal perturbation is not applied directly at the interface, and the ohmic potential drop through the soil electrolyte resistance R_E should be taken into account. Besides, the presence of the double layer capacitance C_d plays a bypass circuit, diverting a substantial proportion of the high frequency AC current transferred to the interface. The equivalent electrical circuit will then be represented by R_E-(C_d//R_p) (cf. Figure 1b on Part I).[1] Therefore, there is a strong coupling between the actual total current flowing across the interface and the overall potential. Main entities that determine the electrical behavior of the interface are, in addition to the reaction rate equations, on one hand the electrolyte resistance, and on the other hand the double layer capacitance.

Montella[9] studied recently the validity of the polarization resistance (R_p) measurements in presence of AC signal by analyzing the nonlinear response to a low frequency sinusoidal voltage perturbation on the electrochemical reaction. He was interested particularly to the maximum voltage amplitude admissible for

*e-mail: hisasi.takenouti@upmc.fr

determining accurately the local polarization resistance. For this sake, he examined an electrochemical system controlled by the activation energy (Tafelian system) at the steady-state in presence of ohmic drop. Since he considered the steady-state conditions, he neglected the contribution of the charging current of the interface capacitance, and then the current-potential response can be modelled by using the Lambert W function.

Though highly interesting, his results cannot be applied to the AC enhanced corrosion of metallic equipment subjected to AC voltage perturbation because of the relatively high range of AC frequency operated on the industrial equipment, typically 16⅔, 50, or 60 Hz, thus the contribution of the charging current of the interface capacitance is no longer negligible.

A model describing the corrosion of metals subjected to its enhancement induced by alternating voltage, taking into account the electrolyte resistance R_E (Ω cm^2) and the double layer capacitance C_d (F cm^{-2}), was developed by Lalvani and his group.[6,7] In their approach, they considered an electrochemical interface controlled by activation processes for both anodic and cathodic reactions (bi-tafelian corrosion mechanism). These authors supplied an approximate solution valid in principle for relatively small amplitude of the AC perturbation. The validity of this approach will be discussed later in this paper.

As explained in Part I,[1] the enhancement of the corrosion current density is due to the faradaic rectification as consequence of nonlinear property of the current-potential characteristics. From a qualitative point of view, the faradaic rectification is always present, and it is significantly influenced by both the electrolyte (solution) resistance R_E and the double layer capacitance C_d.

The complete model, without any approximation will be presented in this Part II for bi-tafelian corrosion mechanism. The anodic dissolution of steel is assimilated to that of iron.

$$\text{Anodic reaction: } Fe \rightarrow Fe^{2+} + 2e^- \quad (1)$$

The cathodic process is the reduction of water molecules.

$$\text{Cathodic reaction: } 2H_2O + 4e^- \rightarrow H_2 + 2OH \quad (2)$$

In Part III, we will deal with the corrosion mechanism where cathodic process is constituted of the reduction of dissolved oxygen partly controlled by diffusion and that of the water following a Tafel law; this mixed mechanism will be named, for simplicity, three reaction corrosion mechanism.

The corrosion current density may be markedly higher than that of the diffusion limiting current density of dissolved oxygen, because of soil aggressiveness, or due to a hindering of the diffusion process by the presence, for instance, of sand at the vicinity of corroding area. In a such case, the diffusion reaction is negligible with respect to the overall cathodic current density. The corrosion mechanism will then be assimilated as a bi-tafelian one. Nonetheless, the corrosion kinetic parameters corresponding to mildly corrosive soil will also be examined, to highlight the difference between bi-tafelian and three reaction corrosion mechanisms. This aspect will be shown in detail in the following paper, Part III of this series.

Experimental

It is worth to recall that, as mentioned in Part I,[1] buried steel pipes are covered by a thick organic coating, and the corrosion protection is completed by the cathodic protection. It also postulated, as in Part I,[1] that the effect of stray AC signal is limited to its kinetic effect, and no side effect such as the modification of soil chemistry close to coating defect, such as pH change or formation of calcareous or magnesium-calcareous deposits will take place. In the corroding system where the electrolyte resistance is no longer considered negligible, the electrode potential E (in V) at the steel/electrolyte interface and the applied potential U (in V) with a reference electrode located at certain distance from the exposed steel area at coating defect are different.

$$E = U - R_E I \quad (3)$$

where I stands for the current density (A cm^{-2}). In presence of an AC strain potential ΔU at the pulsation ω (radian s^{-1}) as a function of time t (s) is expressed by:

$$U = U_0 + \Delta U \sin(\omega t) \quad (4)$$

With several mathematical operations, similar to those presented in Part I, the final equation to be solved, for the corrosion mechanism involving anodic and cathodic reactions, both of them controlled by the activation energy (bi-tafelian corrosion mechanism), can be expressed as follows:

$$U_0 + \Delta U \sin(\omega t) = E(t) + R_E\left\{C_d \frac{dE(t)}{dt} + I_{corr,0}\left[\exp\left\{b_a\left(E(t) - E_{corr,0}\right)\right\} - \exp\left\{b_c\left(E(t) - E_{corr,0}\right)\right\}\right]\right\} \quad (5)$$

In this equation, U_0 represents DC applied potential corresponding to the cathodic protection potential, thus it will be represented also by U_{CP}. The term between braces

is the current passing through the interface involving that of the charge of double layer capacitance, the first term inside the braces.

Before resolving this equation, we will see the validity limit of the so-called "linear approximation" reported by Xiao and Lalvani,[7] regarding specifically the effect of the peak-voltage of AC perturbation, ΔU on the corrosion kinetics.

Results and Discussion

Comparison of linear approximation and fully developed equation on I-U curves under AC perturbation

With linear approximation, the current and potential in presence of the AC perturbation can be expressed analytically, whereas without approximation, digital resolutions are necessary. As presented in Part I,[1] when the electrolyte resistance is neglected, the faradaic rectification can be calculated by using a series of the modified Bessel functions of the first kind of order k (k = 0 to ∞). This is no longer possible in the present situation, then we employed Mathematica® software.[10] This method is rather time consuming, for instance, with a desktop PC equipped with Intel i5-4440 running at 3.1 GHz, two to three hours are necessary to obtain one curve with 500 points. With the linear approximation, one curve is obtained almost instantaneously.

Using digital integration, the mean DC interfacial potential E_{AV} and the capacitive current were evaluated, then the average value of the faradaic anodic and cathodic current ($I_{Fa,AV}$ and $I_{Fc,AV}$, respectively) flowing through the interface were estimated. In the model adopted to simulate the interface, the double layer capacitance is assumed to be equivalent to a pure capacitance, the mean DC capacitive current is therefore nil. Consequently, the mean DC total current transferred to the interface is equal to the sum of the mean DC anodic and cathodic faradaic currents. Hence, the DC mean polarization curves, U_{AV}-I_{AV}, were yielded for different values of the parameters as it was carried out in Part I.[1] The averaged values, marked by subscript "AV" is obtained by integrating through an entire period of the AC signal, both the interfacial potential and the sum of the faradaic anodic and cathodic currents signals.

Table 1 displays some corrosion kinetic parameters used for the comparison of two methods, linear approximation and the complete resolution. These values are essentially the same to those employed in Part I with negligibly small electrolyte resistance.[1]

Figure 1 shows the comparison of the mean DC polarization curves of bi-tafelian corrosion mechanism obtained by the "linear approximation" method[7] and those without approximation by digital resolution. Note that the curve for ΔE = 0 V is the polarization curve for control obtained analytically. These curves allows one to evaluate the faradaic rectification effect on the corrosion potential shift ($\Delta E_{corr,AV} = E_{corr,AV} - E_{corr,0}$) and on the enhancement of corrosion current density ($I_{corr,AV}$).

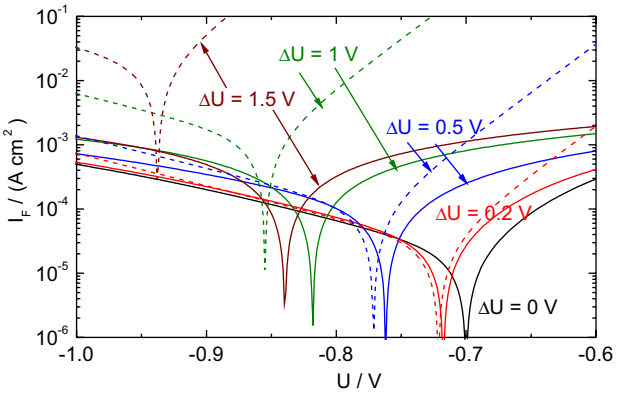

Figure 1. Comparison of polarization curves calculated with the linear approximation (dashed line) and that of full development of equation 5 (solid line). The AC peak voltage ΔU is indicated near each curve. The corrosion parameters used are displayed in Table 1.

It can be seen that, with linear approximation (Figure 1, dashed line), the anodic and cathodic reaction rates keep the same Tafel constant (expressed as V^{-1}) whatever the value of the peak voltage of the AC perturbation. In other terms, if the correction of the ohmic drop term ($E = U - R_E I_F$) was applied, not illustrated here, the Tafel slope becomes steeper, when ΔU increases. Even, for high current density, the polarization curves exhibit an overhanging shape "⊂" for cathodic branch and that of "⊃" shape for anodic branch. In other terms, two different current densities can be observed for a given

Table 1. Values of some corrosion kinetics parameter used for calculating I-U curves and several useful parameters

$E_{corr,0}$ / V	$I_{corr,0}$ / (μA cm^{-2})	b_a / V^{-1}	b_c / V^{-1}	R_E / (Ω cm^2)	C_d / (μF cm^{-2})
–0.7	20	38.3	–12.8	100	100
f / Hz	R_p / (Ω cm^2)	$R_p I_{corr,0}$ / V	$2\pi f R_E C_d$ dimensionless	$(R_E + R_p)/R_p$ dimensionless	r dimensionless
50	978	0.0196	3.14	1.102	1/3

$E_{corr,0}$: corrosion potential without AC signal; $I_{corr,0}$: corrosion current density without AC signal; b_a: Tafel constant for anodic reaction; b_c: Tafel constant for cathodic reaction; R_E: electrolyte resistance; C_d: double layer capacitance; f: frequency of AC signal; R_p: polarisation resistance ; r: $-b_c/b_a$.

potential, i.e., multiplicity of the steady states leading to an instability of the system under potential regulation. The ohmic drop allowed the stabilization of the system.[11]

On the contrary, with the calculation without approximation (solid line), the Tafel slope becomes significantly gentler when ΔU becomes greater. If the ohmic drop correction was applied, these curves show the Tafel constants for anodic and cathodic reactions (b_a and b_c, respectively), almost equal to those used for simulation calculations. One may remark also that, in presence of AC signal, the linear approximation overestimates markedly the corrosion potential shift and the corrosion current enhancement for high ΔU values. These effects are illustrated in more detail in Figure 2.

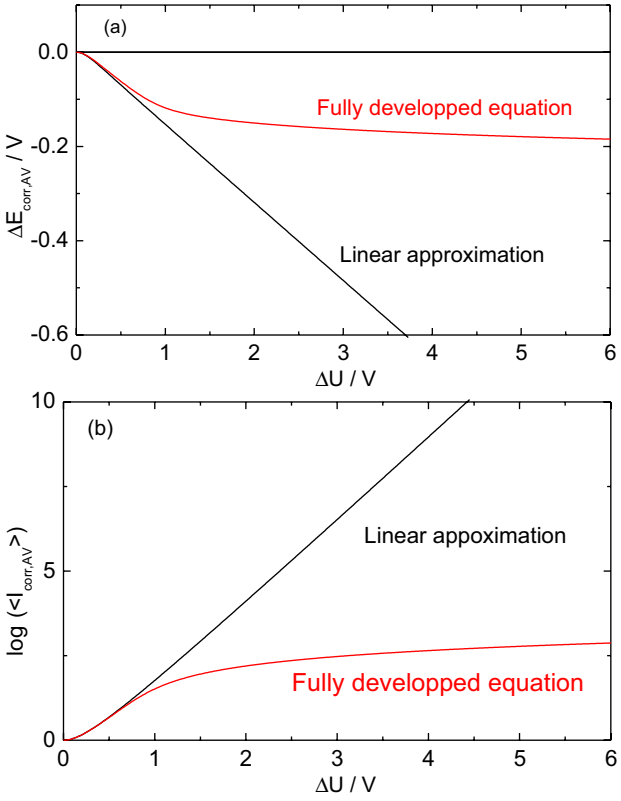

Figure 2. Comparison of the corrosion potential shift in (a) and the enhancement of the corrosion current density in (b) for simulated data obtained by the two approaches, linear approximation and full development of equation 5.

The dependence of the corrosion potential shift $\Delta E_{corr,AV}$, with respect to the peak voltage ΔU, for the two calculation methods, are shown in Figure 2a. It may worth to recall that, since the overall DC current is naught at the corrosion potential even in presence of the AC perturbation, $U_{corr,AV} = E_{corr,AV}$. The corrosion potential shift $\Delta E_{corr,AV}$ is defined as:

$$\Delta E_{corr,AV} = E_{corr,AV} - E_{corr,0} \quad (6)$$

It can be seen that with the linear approximation, the corrosion potential decreases linearly above ΔU > 0.2 V whereas the complete resolution of equation 3 without approximation showed an inflexion point at about ΔU = 1 V. Above this point, the $\Delta E_{corr,AV}$ variation is significantly slower with respect to ΔU.

Figure 2b shows the enhancement of the corrosion current density in presence of AC signal. In this Figure, the corrosion current density is normalized according to the following equation:

$$<I_{corr.AV}> = \frac{I_{corr,AV}}{I_{corr,0}} \quad (7)$$

For ΔU > 0.2 V, the corrosion current density increases exponentially (linear in semi-logarithmic scale) when evaluated by the linear approximation. On the contrary, when it was determined by digital simulation without approximation, two curves overlap almost up to ΔU ca. 0.7 V, then diverge each other. The slope of log ($<I_{corr,AV}>$) changes at about ΔU = 1 V, approximately at the same potential for ΔU – log ($<I_{corr,AV}>$) and ΔU – $\Delta E_{corr,AV}$ curves. At ΔU = 6 V, $I_{corr,AV}$ is increased by 750 times with respect to $I_{corr,0}$, according to the fully developed equation. The overestimation of the corrosion current density under AC voltage enhancement between two calculation methods is illustrated in Figure 3.

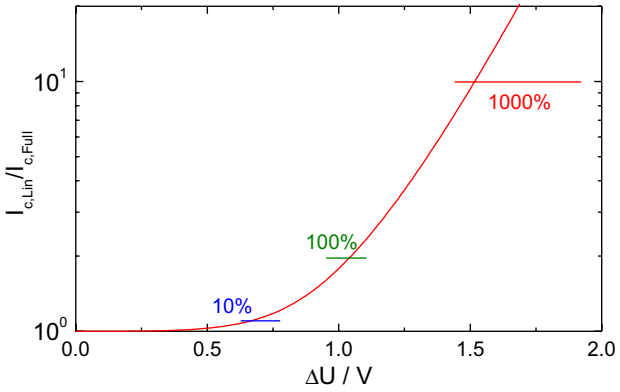

Figure 3. Comparison of corrosion current density evaluated by two methods with respect to the amplitude of AC signal. The horizontal bars indicate the overestimation of corrosion current density by linear approximation.

In Figure 3, $I_{c,Lin}$ and $I_{c,Full}$ represent, respectively, the averaged corrosion current density evaluated by linear approximation according to Xiao and Lalvani[7] and that by numerically resolving equation 5. It can be remarked that the overestimation by linear approximation reaches 10% at ΔU = 0.67 V, twice as much at 1.05 V, and ten times as great at 1.52 V. If the maximum error induced by the linear model is fixed arbitrary at 10%, the use of this method will be limited to ΔU = 0.67 V. AC peak-voltage of several volts

Table 2. Values of some corrosion kinetic parameters used for calculating I-U curves for mildly aggressive corrosive medium

$E_{corr,0}$ / V	$I_{corr,0}$ / (μA cm^{-2})	b_a / V^{-1}	b_c / V^{-1}	R_E / (Ω cm^2)	C_d / (μF cm^{-2})
–0.75	4	23.1	–19.2	200	100
f / Hz	R_p / (Ω cm^2)	$R_pI_{corr,0}{}^a$ / V	$2\pi fR_EC_d$ dimensionless	$(R_E + R_p)/R_p$ dimensionless	r dimensionless
50	5910	0.0236	6.28	1.034	5/6

$E_{corr,0}$: corrosion potential without AC signal; $I_{corr,0}$: corrosion current density without AC signal; b_a: Tafel constant for anodic reaction; b_c: Tafel constant for cathodic reaction; R_E: electrolyte resistance; C_d: double layer capacitance; f: frequency of AC signal; R_p: polarisation resistance ; r: $-b_c/b_a$.

is sometimes encountered in the field measurements. In other terms, for a reasonable evaluation of the corrosion enhancement in presence of AC signal, the use of the complete mathematical resolution by digital simulation is necessary.

AC corrosion enhancement with complete mathematical resolution

Using the numerical resolution of the differential equation related to the instantaneous interfacial potential, we will illustrate, now, the faradaic rectification induced on the corrosion of steel pipeline buried in a mildly or a highly aggressive soil. The difference between them is characterized mainly by the corrosion current density in absence of AC signal $I_{corr,0}$, and by the electrolyte resistance R_E of the soil.

Case 1: mildly aggressive soil

The corrosion kinetic parameters used for the digital simulation for a mildly aggressive soil are grouped in Table 2. These values were mainly determined from the field experiences collected by the French gas and electricity utility company (GDFSUEZ). The results of simulation calculation will be shown first for the corrosion kinetic parameters presented in Table 2, then in reduced variables to be applied for more general cases.

Presentation with particular value of parameters

The corrosion current density of 4 μA cm^{-2} corresponds to the thickness-loss of steel, by uniform corrosion, of 46 μm y^{-1}. The electrode impedance according to the corrosion kinetic parameters displayed in Table 2 is presented in Figure 4 in the Nyquist plot. On this Figure, the frequency of AC signal f adopted (50 Hz) leading to the corrosion enhancement is indicated with an arrow in the insert corresponding to the high frequency part of the impedance in enlarged scale. It can be noticed that at this frequency, the impedance is essentially determined by the electrolyte resistance R_E and double layer capacitance C_d. The real part due to the contribution of the faradaic impedance represented by the diameter of the Nyquist plot is negligibly small (0.27 over 5927 Ω cm^2).

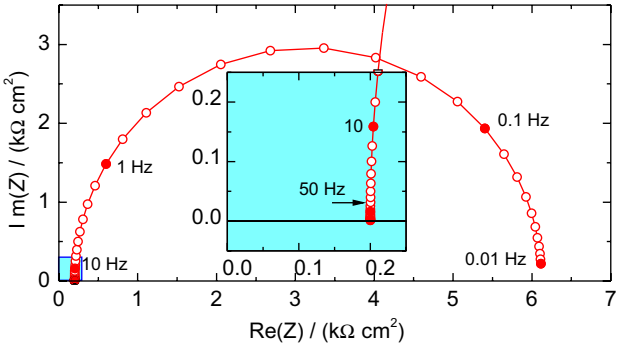

Figure 4. Impedance spectrum of corroding steel electrode in a mildly aggressive corrosive soil. Some frequencies in Hz are indicated near the impedance diagram. The corrosion kinetic parameters are presented in Table 2.

Figure 5 shows the polarization curves obtained for various ΔU values with solid lines. It can be remarked that, under the influence of the AC voltage perturbation, the Tafel constant (b in V^{-1}), in absolute value, decreases when ΔU becomes greater (i.e., gentler Tafel slope), for both anodic and cathodic processes, as indicated above for Figure 1. As mentioned above, once the ohmic potential drop was corrected, the Tafel constants of anodic and cathodic

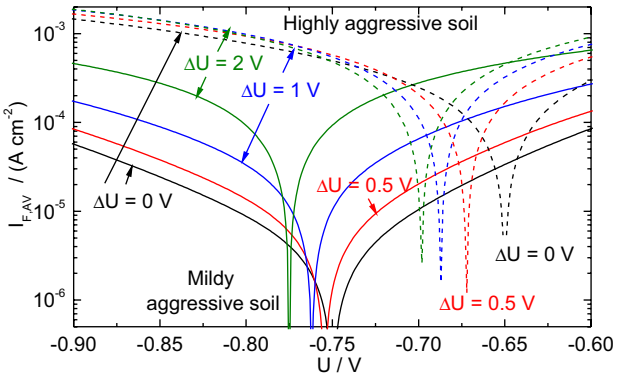

Figure 5. Digitally simulated polarization curves modified by faradaic rectification with various ΔU values (indicated with arrows). Solid lines for mildly aggressive soil with the corrosion kinetic parameters in Table 2, and dashed lines for highly aggressive soil with the corrosion kinetic parameters in Table 3.

branches are almost equal to those given in Table 2. On the other hand, it can be seen, as expected, that $E_{corr,AV}$ shifts towards more negative values since $b_a > -b_c$, and $I_{corr,AV}$ increases with ΔU as predicted in Part I, where the contribution of the electrolyte resistance was neglected.[1]

How the faradaic rectification will be related to the double layer capacitance C_d, and how it will be simultaneously influenced by the corrosion current density $I_{corr,0}$ determined without AC signal? These effects are illustrated in Figure 6.

Figure 6A depicts the variation of the corrosion potential $\Delta E_{corr,AV} = E_{corr,AV} - E_{corr,0}$ with respect to the AC amplitude ΔU. The corrosion potential shift $\Delta E_{corr,AV}$ decreases steeply at low ΔU, then markedly slowly (Figure 6A, curve a) as it was observed in Figure 2a. The double layer capacitance C_d is linked in parallel, and then this element intervenes in the faradaic rectification. When C_d value is increased, from 100 to 250 μF cm², the corrosion potential shift is presented by curve b in Figure 6A. Actually, one observes that the same $\Delta E_{corr,AV}$ is obtained for higher ΔU as indicated by an arrow. The double layer capacitance shunts the AC perturbation, and then the actual perturbation signal at the interface becomes smaller.

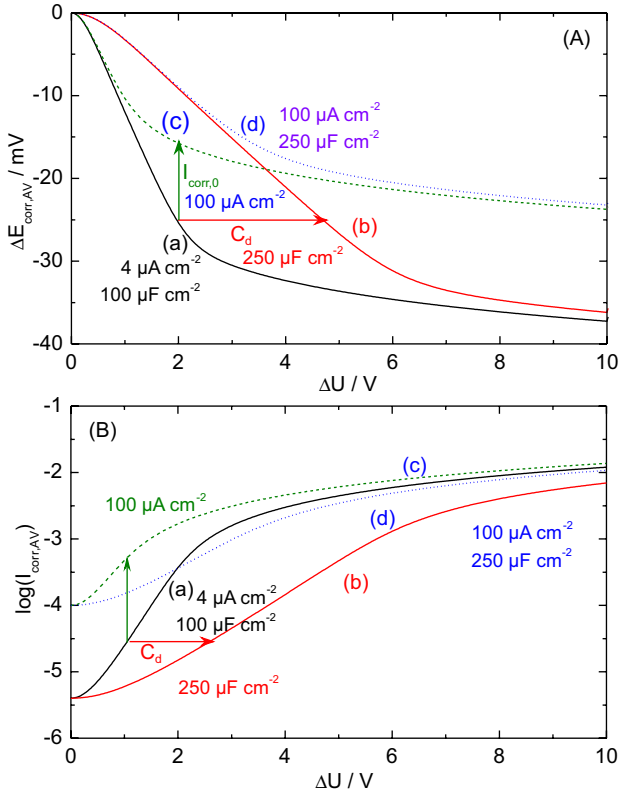

Figure 6. Effects of $I_{corr,0}$ and C_d on corrosion potential shift in (A) and the corrosion current density in (B) induced by faradaic rectification under AC perturbation. Curve identification: (a) $I_{corr,0}$ = 4 μA cm⁻², C_d = 100 μF cm⁻²; (b) $I_{corr,0}$ = 4 μA cm⁻², C_d = 250 μF cm⁻²; (c) $I_{corr,0}$ = 100 μA cm⁻², C_d = 100 μF cm⁻²; (d) $I_{corr,0}$ = 100 μA cm⁻², C_d = 250 μF cm⁻² (other kinetic constants are expressed in Table 2).

One may remark also that these two curves approaches when ΔU increases. At high ΔU, the current density becomes greater, that is, the mean polarization resistance $R_{p,AV}$ (= $\Delta U/\Delta I_{AV}$) becomes smaller. The actual AC amplitude at the interface will then diminishes due to the "bypass" effect brought about by the circuit constituted of R_E–C_d//$R_{p,AV}$.

Now, let us see the effect of the corrosion current density. When $I_{corr,0}$ is increased from 4 to 100 μA cm⁻², the results of calculation are presented by curves a and c in Figure 6A. The difference of $\Delta E_{corr,AV}$ between these two curves is small at low ΔU. However, the difference appears clearly when ΔU becomes greater than 1 V. At low ΔU, C_d plays predominant role on the faradaic rectification, whereas at high ΔU, $R_{p,AV}$ becomes smaller, then it comes to impact on $E_{corr,AV}$, leading to a decrease of the corrosion potential shift. If C_d and $I_{corr,0}$ both increase (from 100 to 250 μF cm⁻² and 4 to 100 μA cm⁻², respectively), the comparison of curves a and d in Figure 6A shows the combination of both effects, as observed on individual effect of these two parameters.

Now, let us see the influence of the peak AC amplitude, ΔU, on the averaged corrosion current density $I_{corr,AV}$ due to the faradaic rectification. As the increase of this current density is rather huge, several orders of magnitude, we will present it in logarithmic scale. Curve a (Figure 6B) shows S-shaped feature. log ($I_{corr,AV}$) increases slowly for small ΔU values, up to ΔU ca. 0.2 V, then linearly to ΔU ca. 2.5 V in semi-logarithmic scale. Beyond this AC potential, the increase of $I_{corr,AV}$ becomes slower. When C_d is increased from 100 to 250 μF cm² (curve b, Figure 6B), the slope of log ($I_{corr,Av}$) – ΔU is much gentler indicating a smaller corrosion enhancement effect of the faradaic rectification. Now, if $I_{corr,0}$ is increased, from 4 to 100 μA cm⁻², curve c in Figure 6B exhibits almost parallel shift with respect to curve a in Figure 6B (in semi-logarithmic scale) up to ΔU ca. 1 V, and beyond this value the two curves approach. The same remark can be formulated when both $I_{corr,0}$ and C_d are augmented. The contribution of C_d to the faradaic rectification is therefore strongly dependent on the averaged current density flowing through the interface, since this capacitance is linked in parallel to $R_{p,AV}$, which becomes smaller with the increase of $I_{corr,AV}$. Note that, when the corrosion process progresses, an accumulation of corrosion products, namely, carbon, iron oxides, and manganese ones, leads to an increase of the true surface area of electrolyte/electronic conducting species, sometimes called as roughness factor, consequently the C_d value becomes greater. With time, therefore, $\Delta I_{corr,AV}$ becomes smaller for a given ΔU as can be noticed by the comparison of curves a and b in Figure 6B.

In what extent the cathodic protection will be effective in presence of AC signal? Figure 7 presents the partial

anodic contribution in the total faradaic current density $I_{Fa,AV}$ for various AC amplitudes. The open circuit corrosion potential and the corrosion current density without AC signal ($E_{corr,0}$, $I_{corr,0}$) are indicated by a dot on this Figure.

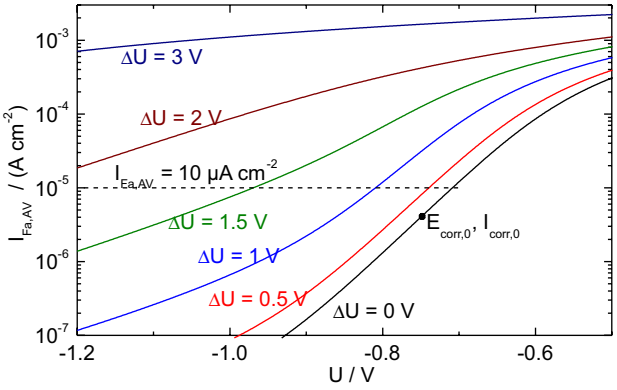

Figure 7. Averaged faradaic anodic components $I_{Fa,AV}$ in presence of AC signal of various amplitudes to illustrate the theoretical DC cathodic protection potential that would be necessary to mitigate the AC corrosion of carbon steel in mildly aggressive soil for the bi-tafelian corrosion model.

As stated above, it was postulated in this calculation no change of the electrochemical parameters characterizing the steel/soil interface induced by the corrosion process itself. If, arbitrarily, the maximal admissible DC anodic faradaic current density $I_{Fa,AV}$, i.e., the corrosion current density under cathodic protection, is assumed to be 10 μA cm^{-2}, which corresponds to a uniform thickness-loss of 116 μm y^{-1}, cathodic protection potential (U_{CP}) of ca. –1 V is necessary for ΔU = 1.5 V and more than –1.2 V for ΔU = 2 V. For higher amplitude of AC signal (for instance ΔU = 2.5 V), an efficient cathode protection (according to the protection criteria arbitrarily considered here) is no longer possible, because in the cathodic range beyond U_{CP} = –1.2 V the hydrogen evolution reaction becomes the major cathodic process, i.e., the cathodic current density becomes higher than 1.5 mA cm^{-2} when U_{CP} is in the range of U_{CP} = –1.2 V. This high rate of hydrogen evolution reaction in presence of the AC perturbation may make the soil pH at the vicinity of corroding area highly alkaline, and may prevent any stabilization of an iron oxide protecting layer at steel surface. This aspect of the AC corrosion mitigation challenge on coated and cathodically protected underground pipelines will be specifically addressed in Part IV of this series of papers.

Faradaic rectification effects in generalized presentation

As in Part I, we will calculate the faradaic rectification effect with dimensionless variables.[1] For practical use of these Figures (8, 9, 11, and 12) for a given system, therefore, it is sufficient to determine, in absence of AC signal, the corrosion parameters ($I_{corr,0}$, $E_{corr,0}$, b_a, and b_c) which allow converting Figures below (8, 9, 11, and 12) to dimensioned curves, in V and A cm^{-2}.

The dimensionless peak voltage of AC perturbing signal <ΔU> was represented by dividing ΔU by so called Stern-Geary coefficient B_{SG}.[12]

$$<\Delta U> = \frac{\Delta U}{B_{SG}} \text{ where } B_{SG} = R_p I_{corr,0} = \frac{1}{b_a - b_c} \qquad (8)$$

In the example given here, if the corrosion current density without AC signal is fixed to be equal to the case illustrated above, B_{SG} remains constant and equal to 23.6 mV. Besides, instead of individual Tafel constants, their ratio r was used.

$$r = -\frac{b_c}{b_a} \qquad (9)$$

Note that the value of r is positive.

The reduced corrosion potential shift $<\Delta E_{corr,AV}>$ in presence of AC signal was defined as follows:

$$<\Delta E_{corr,AV}> = \frac{E_{corr,AV} - E_{corr,0}}{\Delta U} \qquad (10)$$

Figure 8 illustrates the effect of r ratio on the corrosion potential shift. In this calculation, the kinetic constants used correspond to those presented in Table 2 except for the two Tafel constants b_a and b_c.

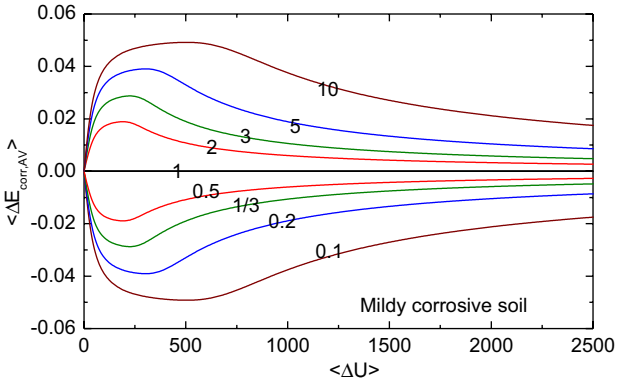

Figure 8. The variation of dimensionless corrosion potential shift $<\Delta E_{corr,AV}>$ in a mildly aggressive soil with respect to the reduced AC amplitude <ΔU> for various r values indicated as parameter. Corrosion kinetics parameters are those given in Table 1 except b_a and b_c, but ($b_a - b_c$) was kept constant. B_{SG} = 23.6 mV.

On Figure 8, it can be noticed firstly that $<\Delta E_{corr,AV}>$ are symmetrical for r and 1/r with respect to the <ΔU>-axis as it was also reported in Part I for bi-tafelian corrosion mechanism.[1] Secondly, these curves exhibit a peak which

was not observed in Part I where the electrolyte resistance and consequently the double layer capacitance were neglected.[1] No such behavior was observed neither in Figure 2a with fully resolved equation 5 expressed with the dimensioned variables. The peak observed is, indeed, only due to the fact that these curves are presented with respect to dimensionless variables, according to equation 8 and equation 10. If $<\Delta E_{corr,AV}>$ was multiplied by ΔU, i.e., dimensioned magnitude, monotonically decreasing (when r < 1) or increasing (when r > 1) curves, were observed. As this was the case also in Part I, when r = 1, no corrosion potential shift was observed.[1] It can also be noted that more asymmetrical the polarization curve is, the greater the corrosion potential shift is.

Figure 9 shows the relative variation of the reduced corrosion current density, $<I_{corr,AV}>$, for various r values with respect to the normalized peak amplitude of AC signal <ΔU>.

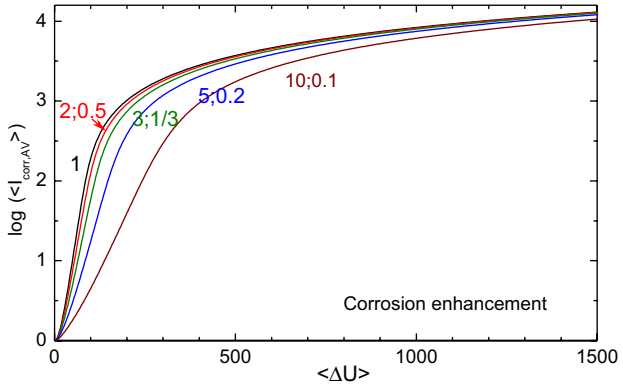

Figure 9. Effect of faradaic rectification on the averaged corrosion current density, $<I_{corr,AV}> = I_{corr,AV}/I_{corr,0}$ with various $-b_c/b_a$ ratios with respect to the dimensionless AC amplitude (corrosion parameters are expressed in Table 2, except for b_a and b_c but ($b_a - b_c$) is kept constant). B_{SG} = 23.6 mV.

As it was observed in Part I for the system for bi-tafelian mechanism with a negligibly small electrolyte resistance, the most marked corrosion enhancement was observed for r = 1.[1] Also, as observed in Part I, when considering a given r ratio value and its reciprocal value (1/r), the two curves are completely superimposed. On this Figure, one can remark also an inflexion point depending on the r ratio. These curves are different to those observed in Part I where the electrolyte resistance R_E is neglected. Indeed $<I_{corr,AV}>$ increased linearly with <ΔU>.[1] The ohmic drop term and the attenuation of AC signal make therefore the corrosion enhancement smaller. For high <ΔU> values, the corrosion current enhancement with increasing values of <ΔU> attenuate markedly. The electrolyte resistance shows therefore a beneficial effect on the AC induced corrosion.

Now, let us see the faradaic rectification effects on steel pipe buried in a highly aggressive soil.

Case 2: highly aggressive soil

The kinetic constants used for this system, based upon the field experiments, are given in Table 3. In this Table, it can be noticed that the "free corrosion" current density is considered as 37.5 times as great as in a mildly corrosive medium presented above. In other terms, the corrosion rate corresponds to 1.74 mm y^{-1} for the uniform thickness loss. The open circuit corrosion potential is 0.1 V more positive, and b_a is ca. 1.66 fold greater than that used in a mildly aggressive soil. The solution resistance is slightly smaller whereas the double layer capacitance is 1.5 times as great.

Presentation with particular value of parameters

The polarization curves obtained by digital summations of equation 5 are superimposed in Figure 5 above. It is important to emphasize that, in the conditions used here, ΔU has no significant effect on the faradic rectification for high overvoltage. All curves tend to overlap for U < –0.75 or U > –0.4 V (not illustrated here). The anodic or cathodic reaction rate becomes faster, then $R_{p,AV}$ becomes smaller. As a result, the amplitude ΔU of the AC perturbation is damped essentially through the electrolyte resistance. The effective AC amplitude ΔE at the steel/electrolyte interface becomes therefore small. In this steady-state plot, the double layer capacitance does no longer intervene markedly in the electrical characteristics, and then only the electrolyte resistance and the polarization resistance are linked in series. For instance, for the slope of polarization curve, $I_{F,AV}$-U (Figure 5) at the current density equal to 1 mA cm^{-2}, for ΔU = 2 V, one yields the apparent polarization resistance at the interface $R_{p,AV}$ = 14.8 Ω cm^2. The effective amplitude

Table 3. Values of some corrosion kinetic parameters and pertinent ones used for calculating I-U curves for highly aggressive corrosive medium

$E_{corr,0}$ / V	$I_{corr,0}$ / (μA cm^{-2})	b_a / V^{-1}	b_c / V^{-1}	R_E / (Ω cm^2)	C_d / (μF cm^{-2})
–0.65	150	38.4	–19.2	100	150
f / Hz	R_p / (Ω cm^2)	$R_pI_{corr,0}{}^a$ / V	$2\pi fR_EC_d$ dimensionless	$(R_E + R_p)/R_p$ dimensionless	r dimensionless
50	115.7	0.0174	6.28	1.086	1/2

$E_{corr,0}$: corrosion potential without AC signal; $I_{corr,0}$: corrosion current density without AC signal; b_a: Tafel constant for anodic reaction; b_c: Tafel constant for cathodic reaction; R_E: electrolyte resistance; C_d: double layer capacitance; f: frequency of AC signal; R_p: polarisation resistance; r: $-b_c/b_a$.

of AC signal, ΔE is 12.8% of applied ΔU, i.e., ΔE = 0.26 V. When ΔU = 3 V at the same potential (–0.802 V), the $I_{F,AV}$ is –0.93 mA cm^{-2} and the slope of the polarization curve gives the polarization resistance, including the electrolyte resistance equal to 105.8 Ω cm^2. Then the $R_{p,AV}$ is evaluated to 5.8 Ω cm^2. Thus, 5.5% of applied AC signal is effectively modulating the interface potential, i.e., 0.165 V. Because of higher corrosion enhancement, the effective AC signal is surprisingly small in this case. This is why the averaged current density depends little beyond $I_{F,AV}$ equal to 1 mA cm^{-2}.

Figure 10 presents the anodic component of the averaged current density in presence of various AC amplitudes. The open circuit condition without AC signal in this highly aggressive soil is indicated by a dot. As above, if the admissible current density is arbitrarily assumed to be equal to 10 μA cm^{-2}, one can see that, upon this protection criteria, U_{CP} of ca. –0.8 V will be necessary to protect the steel pipe from the corrosion in absence of AC signal. At U_{CP} = –1.2 V, the cathodic protection will be efficient up to ΔU ca. 0.75 V.

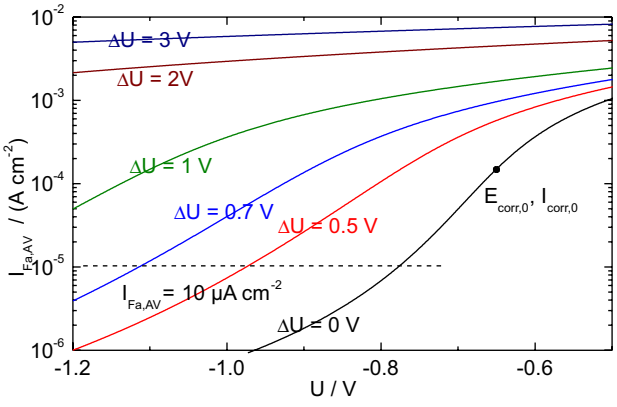

Figure 10. Averaged faradaic anodic components in presence of AC signal of various amplitudes to illustrate the cathodic protection potential that would be necessary to mitigate the AC corrosion of carbon steel in highly aggressive soil.

We will see now AC corrosion enhancement with reduced scale to generalize the results of calculations.

Faradaic rectification effects in generalized presentation

Figure 11 shows the reduced corrosion potential shift <ΔE$_{corr,AV}$> under AC perturbation for various r values. As this was the case for a mildly aggressive soil, the <E$_{corr,AV}$> is symmetrical with respect to the <ΔU> axis for two reciprocal values of r. A peak of <E$_{corr,AV}$> change was also observed, and this feature is actually due to the dimensionless presentation used here, that is the potential shift divided by the peak AC amplitude ΔU. If E$_{corr,AV}$ was presented under dimensioned form, a monotonous change was observed.

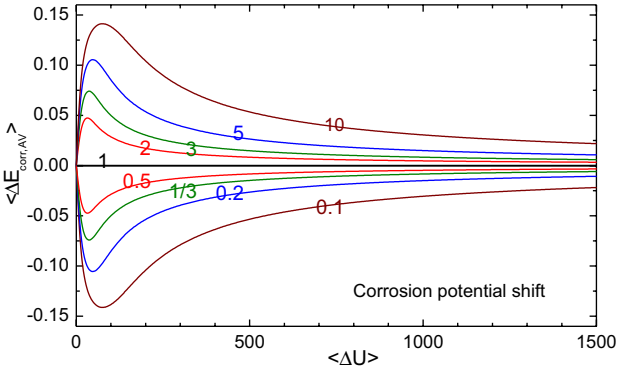

Figure 11. Effect of <ΔU> upon <ΔE$_{corr,AV}$> in a highly corrosive soil for various r ratios. The corrosion kinetic parameters are given in Table 3. B_{SG} = 17.4 mV.

For small <ΔU> values, <ΔE$_{corr,AV}$> is greater when compared with the results illustrated in Figure 8. As can be remarked on Figure 5, the corrosion potential shift for a given ΔU is more marked in highly aggressive soil. From curves a and c of Figure 6A, the increase of C_d from 100 to 150 μF cm^2, may decrease the corrosion potential shift. The increase of $I_{corr,0}$ from 4 to 150 μA cm^2 may induce also the similar effect. Therefore, a greater <ΔE$_{corr,AV}$> change observed in this medium is essentially due to a smaller R_E value used. Indeed, the comparison for the solution with negligible small electrolyte resistance presented in Part I corroborates this remark.[1]

The AC corrosion enhancement induced by the faradaic rectification by AC signal is presented in Figure 12.

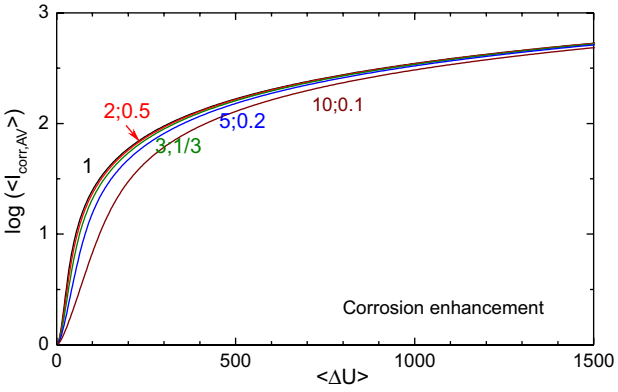

Figure 12. Effect of faradaic rectification with various $-b_c/b_a$ ratios r on the enhancement of the corrosion current, as a function of the peak AC voltage in a highly aggressive soil, with regards to the corrosion process. B_{SG} = 17.4 mV.

The averaged corrosion current density <I$_{corr,AV}$> under AC signal is expressed as above in a dimensionless entity, as can be seen in the equation 7. In semi-logarithmic scale, there are two segments. At low <ΔU>, the reduced corrosion

current increases steeply, then markedly slowly. The transition between these two regimes depends on r value; the higher r (or 1/r) value is, the smaller the threshold amplitude <ΔU> is. For high AC amplitude, all curves tend to join. Compared with a mildly aggressive soil, the corrosion current density induced by AC signal in reduced scale is smaller. R_E value was twice as low in this medium compared with mildly aggressive medium whereas C_d value is 1.5 times greater in a highly aggressive soil. These two last parameters tend to decrease the effective interface perturbing signal ΔE, for a given ΔU value, thus decreasing the corrosion enhancement by the faradaic rectification.

Conclusions

This series of papers addresses the effect of the faradaic rectification phenomenon on the AC enhanced corrosion of buried and coated pipelines located in the vicinity of high voltage AC power lines. The impact of electrical and electrochemical parameters characterizing the steel/soil interface on the AC corrosion kinetics, are theoretically studied. It was assumed that the corrosion kinetics at steel/soil interface at a coating defect is not depending on the time wise development of the corrosion process. The case when the electrolyte resistance R_E is no longer negligible is investigated in this issue. In such a case, the interface capacitance, C_d, contributes also to the corrosion enhancement induced by AC stray potential. In this situation, the contribution of both parameters, R_E and C_d, to the enhanced corrosion kinetics in presence of a high AC voltage is described by an ordinary non-linear differential equation describing the variation of the instantaneous interfacial potential as a function of the time. We did not find any analytical way of resolution of this equation without oversimplification, such as the one proposed by Xiao and Lalvani[7] for low values of the AC voltage perturbation and low values of the mean polarization of the interface with respect to the free corrosion potential.[7] Consequently, the corrosion potential shift and the corrosion enhancement, characterizing the so-called faradaic rectification effect in presence of the AC voltage perturbation, were determined by time-consuming digital simulations.

In this Part II, the case where the corrosion is governed by the bi-tafelian corrosion mechanism is presented. Both R_E and C_d attenuate the AC voltage at the electrode interface ΔE because of the ohmic potential drop and also due to the "bypass effect" exerted by C_d with regards to the faradaic processes. Consequently the AC corrosion enhancement is decreased, when compared with an interface characterized by similar electrochemical parameters, but with the electrolyte resistance being negligibly small.

Xiao and Lalvani[7] proposed an approximate solution of the differential equation for the bi-tafelian corrosion mechanism. For this sake, they used the first order Taylor expansion around the DC average value of the applied AC voltage. With this approximation, they proposed analytical solutions of the differential equations. The validity of this approach was checked by comparing the solutions obtained by digital simulation without approximation. With a reasonable set of corrosion kinetic parameters (see Table 1), there is a significant divergence (10%) as far as the peak voltage ΔU reaches 0.67 V. ΔU measured in field experiments may reach several volts, and much higher voltage was sometimes observed. The linear approximation proposed by Xiao and Lalvani[7] meets hardly the realistic situations. Consequently, though digital resolutions of the corrosion kinetics are time consuming, it is difficult to avoid it.

The effect of the C_d and the corrosion current density $I_{corr,0}$ were checked on the averaged corrosion potential shift $\Delta E_{corr,AV}$, as well as on the enhancement of the averaged corrosion current density $I_{corr,AV}$ induced by faradaic rectification. These averaged values were evaluated by integrating the potential or the current signal over entire periods of AC signal. It was found that for high AC amplitude ΔU, the corrosion potential shift $\Delta E_{corr,AV}$, as well as the corrosion current density $I_{corr,AV}$, change slowly. When the double layer capacitance C_d is increased, $\Delta E_{corr,AV}$ changes less for given ΔU since the impedance modulus of C_d becomes smaller. As for $\Delta I_{corr,AV}$, its increase is less important. With time, the amount of corrosion products such as carbon, iron oxide, and manganese one will increase the steel surface. Then, the double layer capacitance increases with time. As a result, the corrosion enhancement induced by AC signal will decrease. When $I_{corr,0}$ is increased, the $I_{corr,AV} = f(\Delta U)$ curves approaches each other for high ΔU values because the ohmic drop determines the current density. It is worth to emphasize that at $E_{corr,AV}$, the overall current is naught, but the effective AC amplitude of the AC voltage at the interface, ΔE, decreases due to the ohmic drop effect, and when a non-nil overall DC current is flowing through the electrolyte, $I_{F,AV}$-U curve is markedly modified by the presence of non-nil electrolyte resistance.

With dimensionless scale, the set of curves describing the corrosion potential shift, $<\Delta E_{corr,AV}> = (E_{corr,AV} - E_{corr,0})/\Delta U$ and the corrosion enhancement $<\Delta I_{corr,AV}> = (I_{corr,AV}/I_{corr,0})$ with respect to $<\Delta U> = \Delta U/B_{SG}$ are plotted. With these dimensionless representation, one can readily evaluate the effect of any AC voltage perturbation on field systems, by determining E_{corr}, I_{corr}, b_a, and b_c, from the polarization curve close to the open circuit potential in absence of AC signal. These parameters can be obtained easily with

monitoring software of almost all commercial devices by parameter regression procedure. R_E and C_d, also important parameters will be determined by electrochemical impedance spectroscopy technique collected at E_{corr}. The Figures presented in this paper do not allow, however, determining directly their effect, but some interpolation with various Figures presented in this paper may indicate general tendency.

The cathodic protection potential necessary to mitigate the corrosion of buried steel pipe in presence of AC voltage, U_{CP} was tentatively evaluated by plotting the anodic contribution of the overall faradaic current $I_{Fa,AV}$. In this calculation, some restricted hypotheses were used, namely the AC corrosion process itself does not alter the kinetics parameters describing the steel/soil interface behavior. With typical corrosion parameters used in this paper, for mildly aggressive soil, and AC peak amplitude less than 2 V, it appears that U_{CP} values in the range of −1.2 V would be sufficient. In contrast in a highly aggressive soil, with the same U_{CP} values, the cathodic protection would only be efficient for $\Delta U < 0.75$ V.

When the diffusion of dissolved oxygen is negligible compared with the reduction of water molecules, which is the case, for instance, in contact with a highly corrosion aggressive soil or when this cathodic reaction is strongly hindered by the presence of sand close to the defect area, the cathodic reaction due to the reduction of dissolved oxygen is small. In this situation, the cathodic current is essentially determined by the reduction of water leading to the hydrogen evolution validating the corrosion mechanism adopted here, i.e., a bi-tafelian one.

In the next part of this series of papers, we will present the results of digital simulations for the corrosion mechanism involving anodic dissolution obeying a Tafel law, and mixed kinetics for cathodic reactions, one for the reduction of dissolved oxygen partly determined by the convective diffusion and another describing the mechanism of cathodic reduction of water, postulated to follow a Tafel law.

References

1. Ibrahim, I.; Tribollet, B.; Takenouti, H.; Meyer, M.; *J. Braz. Chem. Soc*. **2015**, *26*, 196.
2. Gellings, P. J.; *Electrochim. Acta* **1962**, *7*, 19.
3. Bertocci, U.; *Corrosion* **1979**, *35*, 211.
4. Lalvani, S. B.; Lin, X. A.; *Corros. Sci.* **1994**, *36*, 1039.
5. Lalvani, S. B.; Lin, X.; *Corros. Sci.* **1996**, *38*, 1709.
6. Zhang, R.; Vairavanathan, P. R.; Lalvani, S. B.; *Corros. Sci*. **2008**, *50*, 1664.
7. Xiao, H.; Lalvani, S. B.; *J. Electrochem. Soc.* **2008**, *155*, 69.
8. Bosch, R. W.; Bogaerts, W. F.; *Corros. Sci.* **1998**, *40*, 323.
9. Montella, C.; *J. Electroanal. Chem.* **2012**, *672*, 17.
10. Wolfram, S.; *The Mathematica Book*, 6th ed.; Wolfram Media & Cambridge University Press: Cambridge, 2003.
11. Epelboin, I.; Gabrielli, C.; Keddam, M.; Lestrade, J. C.; Takenouti, H.; *J. Electrochem. Soc.* **1972**, *119*, 1632.
12. Stern, M.; Geary, A. L.; *J. Electrochem. Soc*. **1957**, *104*, 56.

Submitted: August 14, 2015
Published online: November 9, 2015